

# COINCIDENCE, CATEGORIZATION, AND CONSOLIDATION: LEARNING TO RECOGNIZE SOUNDS WITH MINIMAL SUPERVISION

*Aren Jansen, Daniel P. W. Ellis, Shawn Hershey,  
R. Channing Moore, Manoj Plakal, Ashok C. Popat, Rif A. Saurous*

Google Research, Mountain View, CA, and New York, NY, USA

{arenjansen, dpwe, shershey, channingmoore, plakal, popat, rif}@google.com

## ABSTRACT

Humans do not acquire perceptual abilities in the way we train machines. While machine learning algorithms typically operate on large collections of randomly-chosen, explicitly-labeled examples, human acquisition relies more heavily on multimodal unsupervised learning (as infants) and active learning (as children). With this motivation, we present a learning framework for sound representation and recognition that combines (i) a self-supervised objective based on a general notion of unimodal and cross-modal coincidence, (ii) a clustering objective that reflects our need to impose categorical structure on our experiences, and (iii) a cluster-based active learning procedure that solicits targeted weak supervision to consolidate categories into relevant semantic classes. By training a combined sound embedding/clustering/classification network according to these criteria, we achieve a new state-of-the-art unsupervised audio representation and demonstrate up to a 20-fold reduction in the number of labels required to reach a desired classification performance.

**Index Terms**— Sound classification, self-supervised learning, multimodal models, clustering, active learning.

## 1. INTRODUCTION

In the first year of life, typical infants are awake for  $\sim 4000$  hours, during which they are presented with a wide variety of environmental sounds, infant-directed speech, and a companion visual stream of over 1M images (assuming 1 fps). It is only after this pre-verbal exposure that our abilities of object tracking, color discrimination, object recognition, word and phoneme recognition, and environmental sound recognition emerge [1, 2, 3, 4, 5, 6]. Beginning in the second year, children become proficient at knowing what they do not know and solicit explicit labels for novel classes of stimuli they encounter using finger pointing and direct questions [7, 8, 9, 10]. However, this process is not carried out on a per-instance basis; instead, children exploit their past learning of invariances (e.g. rotation/lighting for vision, speaker for speech, loudness for sounds) to generalize a single label from a caregiver to a range of stimuli.

These aspects of early human learning are not captured by the traditional supervised learning practice of collecting a large set of explicitly labeled examples and using it to train a model from scratch. Instead, it is clear humans also rely on some combination of unimodal/multimodal unsupervised learning and active learning to acquire these abilities. With this inspiration, this paper presents a joint learning framework that unites several strands of unsupervised deep learning research to train high quality semantic sound models. As input, we are provided a large collection of unlabeled video data and

the goal is to require only a minimal amount of manual, targeted annotation. Our framework rests on three learning mechanisms: (i) observing coincidences both within and across modalities, (ii) discovering and imposing categorical structure, and (iii) consolidating those categories into practical semantic classes.

Unsupervised learning has undergone major advances with the development of so-called self-supervised learning methods, which define application-specific proxy tasks to encourage neural networks to produce semantically structured representations. We propose a general unimodal and cross-modal representation learning technique based on the proxy task of coincidence prediction, which unifies recent work in audio-only [11] and audio-visual [12, 13] self-supervised learning. The goal is to learn separate audio and image embeddings that can predict whether each sound-sound pair or each sound-image pair occurs within some prescribed temporal proximity in which semantic constituents are generally stable. Each of these two prediction tasks elicits strong semantic encoding and we demonstrate further improvement through their combination.

Once we have a semantically structured representation, we can initiate the discovery of categorical structures that ultimately facilitate connecting our perception to higher-level cognitive reasoning. While any traditional clustering algorithm might apply, we propose a novel, neural network-based clustering procedure that not only provides a partition of the embedding space but also updates the coincidence-trained embedding network to reinforce discovered categories. We demonstrate that this procedure provides further improvements to our embedding model, resulting in a new state-of-the-art unsupervised audio representation.

Finally, automatically discovered categories are not particularly useful until grounded to a prescribed ontology. Traditional active learning methods require access to a pre-existing classifier for prioritization. Absent such a classifier in truly unsupervised settings, we instead adopt a cluster-based active learning procedure [14, 15] whereby we weakly label each discovered category by soliciting an annotation for a randomly selected sound contained within. This neutralizes the sampling hazards of skewed data distributions while functioning to consolidate overly-specialized discovered categories into more meaningful and generalizable classes. Using this targeted annotation procedure, we can obtain weak labels for nearly the entire dataset, which we use to train sound classifiers that are initialized with the unsupervised semantic representation network. The end result is dramatic improvements in classification performance in the usual case where access to explicit supervision is limited.

## 2. RELATED WORK

A wide variety of self-supervised methods have been developed in the audio and computer vision communities. For sound events,

This extended version of a ICASSP 2020 submission under same title has an added figure and additional discussion for easier consumption.

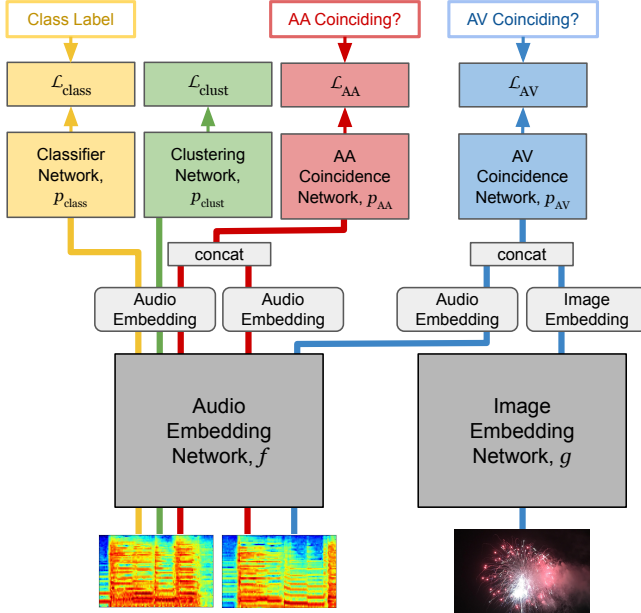


**Fig. 1.** Learning framework diagram. Each of the four loss function processing paths is specified with a color: red for audio-audio (AA) coincidence, blue for audio-visual (AV) coincidence, green for clustering, and yellow for classification.

temporal proximity, temporal lag prediction, context reconstruction, and sound mixing have been demonstrated to be effective [11, 16]. In computer vision, proxy objectives have been based on egomotion [17], spatial/compositional coherence [18, 19, 20], temporal coherence/proximity in video [21, 22], object tracking in video [23], colorization [24], and rotation [25]. The coincidence-based approach we propose directly captures these temporal coherence and proximity criteria. Furthermore, for a sufficiently rich video training dataset in which lighting, camera angle, and object position are all dynamic, coincidence can subsume most of the other listed image-based self-supervised objectives as well.

Recognizing the limitations of unimodal self-supervised methods, researchers have increasingly focused on multimodal training objectives that introduce powerful cross-modal constraints. Three prominent deep learning approaches are (i) Deep Canonical Correlation Analysis (DeepCCA) [26], a deep learning generalization of linear CCA; (ii) Look, Listen, and Learn ( $L^3$ ) [12], which learns representations that can predict audio-visual frame correspondence in videos; and (iii) metric learning losses applied to shared multimodal embedding spaces [27, 28, 29, 30]. In all three cases, the learning is driven by the powerful cue of coincidence of semantic content present in parallel observations across the modalities.

Cluster-based active learning in fixed representation spaces has been proposed in past research [14, 15]. However, to the best of our knowledge, ours is the first attempt to train a neural network with a cluster-based objective to facilitate an active learning procedure. There have also been recent attempts at neural-based clustering [31, 32, 33]. However, each one of those methods reinforces classical k-means solutions, while our proposed approach performs the clustering from scratch, entirely within the context of neural network training.

### 3. THE LEARNING FRAMEWORK

Our goal is to train a single deep audio embedding network that defines a map  $f : \mathbb{R}^{F \times T} \rightarrow \mathbb{R}^d$  from sounds (represented by log mel spectrogram context windows with  $F$  frequency channels and  $T$  frames) to a  $d$ -dimensional representation that supports sound recognition and retrieval tasks. We use a combination of three learning mechanisms, each involving their own auxiliary networks and losses, described in turn below.

#### 3.1. Generalized Coincidence Prediction

Our coincidence prediction approach is based on the assumption that the set of semantic categories we interact with changes much more slowly than the raw pixels and sounds we perceive on an instant-by-instant basis. Therefore, there must exist a relatively stable latent representation of the raw inputs that reflects semantic content and ignores higher frequency extrinsic variation. Such a representation would facilitate prediction of whether a pair of inputs are coinciding, since temporal proximity would be correlated with semantic similarity. Coincidence prediction then becomes a proxy task for semantic representation learning. Critical to this proxy task is the choice of a suitable time scale of coincidence, which we denote  $\Delta T$ . The appropriate value is task-dependent and needs to correspond roughly to the rate of semantic change in the input. Our prior work in temporal proximity-based metric learning [11] was a direct attempt to leverage coincidence for audio representation learning. There, we learned a representation in which spatial proximity was correlated with temporal proximity ( $\Delta T = 10$  s) of the inputs, which elicited useful semantic structure in the embedding space. Our present goal is to extend that approach into a single methodology that can also exploit cross-modal audio-visual self-supervision.

Our coincidence prediction approach is a generalization of the audio-visual (AV) correspondence proxy task [12]. That work’s key innovation was to simultaneously train an audio and image embedding network on unlabeled video that supported prediction of whether an audio and image frame occurred at the same (corresponding) point in time. We introduce three modifications to the that recipe. First, since it is clear from human experience that we need not see an object make a sound to associate them semantically, we relax the time scale in what we call a less restrictive coincidence prediction. Second, we use the same coincidence prediction strategy to exploit both unimodal (audio-audio, for which correspondence is not useful) and cross-modal input pairs to train a single shared audio embedding model. Finally, we improve optimization (and ultimately performance) by exploiting all non-coincident pairs in each minibatch (rather than a single random selection).

As depicted in the red path of Figure 1, our audio-audio (AA) coincidence prediction task is trained on a large collection of coincidence-labeled audio example pairs of the form  $(x_1, x_2, y)$ , where each  $x_i \in \mathbb{R}^{F \times T}$ , and  $y \in \{0, 1\}$  is a coincidence indicator for a time scale  $\Delta T$ . Each audio example is passed through the audio embedding network  $f$ , and the outputs are concatenated into a vector  $z = [f(x_1), f(x_2)] \in \mathbb{R}^{2d}$ . The AA coincidence prediction task is performed by a fully connected binary classification network  $p_{AA} : \mathbb{R}^{2d} \rightarrow [0, 1]$  that maps each  $z$  into the probability that the input pair was coinciding. Given a batch of coinciding example pairs  $X = \{(x_1^{(i)}, x_2^{(i)})\}_{i=1}^B$ , we construct  $B \cdot (B - 1)$  negative examples by assuming each pair  $(x_1^{(i)}, x_2^{(j)})$  for  $i \neq j$  are non-coinciding. This all-pairs construction introduces negligible label noise and uses each mini-batch completely without having to resort to within mini-batch mining techniques required by triplet loss methods [11]. The re-

sulting AA coincidence loss function is the balanced cross-entropy, given by

$$\mathcal{L}_{AA}(X) = -\frac{1}{B} \sum_{i=1}^B \log p_{AA}([f(x_1^{(i)}), f(x_2^{(i)})]) - \frac{1}{B(B-1)} \sum_{\substack{1 \leq i, j \leq B \\ j \neq i}} \log [1 - p_{AA}([f(x_1^{(i)}), f(x_2^{(j)})])]. \quad (1)$$

The AV coincidence prediction task (blue path in Figure 1) operates similarly with three differences. First, each coincidence-labeled training pair  $(x_1, x_2, y)$  now has  $x_2 \in \mathbb{R}^{W \times H \times D}$ , each  $W \times H$  pixel images color depth  $D$ . Second, the image inputs are processed by their own embedding network  $g: \mathbb{R}^{W \times H \times D} \rightarrow \mathbb{R}^d$ , which is jointly trained alongside  $f$ . Third, we introduce a dedicated second AV coincidence prediction network  $p_{AV}$ . The AV coincidence loss function takes the form

$$\mathcal{L}_{AV}(X) = -\frac{1}{B} \sum_{i=1}^B \log p_{AV}([f(x_1^{(i)}), g(x_2^{(i)})]) - \frac{1}{B(B-1)} \sum_{\substack{1 \leq i, j \leq B \\ j \neq i}} \log [1 - p_{AV}([f(x_1^{(i)}), g(x_2^{(j)})])]. \quad (2)$$

This is the same loss form of Equation 1, but with  $p_{AA}$  and  $f(x_2)$  replaced with  $p_{AV}$  and  $g(x_2)$ , respectively.

### 3.2. Categorization with Entropy-based Clustering

We posit that a good clustering is a partition of data points such that (i) each data point is confidently assigned to one cluster, (ii) all available clusters are used, and (iii) the set of points assigned to the same clusters are close under some relevant metric (Euclidean or otherwise). To learn such a  $K$ -way partition, we introduce a map  $p_{\text{clust}}: \mathbb{R}^d \rightarrow [0, 1]^K$  from our embedding space to a categorical distribution specifying the probability of assignment to each cluster (see the green path in Figure 1). We can encourage confident assignment by reducing per-data-point entropy of  $p_{\text{clust}}$ . However, to prevent the trivial solution that assigns all points to one cluster, we must add a countervailing objective that increases the entropy of the  $p_{\text{clust}}$  distribution averaged over the whole dataset. Finally, by expressing the map  $p_{\text{clust}}$  with a neural network of limited complexity, we ensure preservation of locality.

These objectives are amenable to stochastic gradient descent optimization using audio example mini-batches  $X = \{x_i\}_{i=1}^B$ , where each  $x_i \in \mathbb{R}^{F \times T}$ , and the loss function

$$\mathcal{L}_{\text{clust}}(X) = \frac{1}{B} \sum_{i=1}^B H[p_{\text{clust}}(f(x_i))] - \gamma H \left[ \frac{1}{B} \sum_{i=1}^B p_{\text{clust}}(f(x_i)) \right],$$

where  $f$  is the audio embedding map defined above,  $H[\cdot]$  denotes entropy, and  $\gamma$  is a diversity hyperparameter. Increasing  $\gamma$  encourages a more uniform cluster occupancy distribution and, given sufficiently large  $K$ , is the primary setting for model selection. For the special case of  $\gamma = 1$ , minimizing  $\mathcal{L}_{\text{clust}}$  reduces to maximizing the mutual information (MI) between the model inputs and the output clusters, which was previously introduced as a discriminative clustering objective [34]. As that work indicated, MI maximization alone finds trivial solutions, which they address with explicit regularization

terms, but they still required k-means initialization for successful application. Setting our hyperparameter  $\gamma > 1$  also acts to prevent trivial solutions. Critically, however, our objective is amenable to cold start training and can be used to fine tune embedding networks, where the representation evolves during optimization.

### 3.3. Consolidation with Cluster-based Active Learning

Given an imperfect semantic representation, each class will be subject to some degree of fragmentation into multiple modes, while some classes will fail to split into separable structures. Thus, one tenable categorization strategy is to over-partition the space such that hypothesized units remain pure and over-specialized. In this case the final requirement of learning semantic classes is a consolidation, or grouping, of the discovered categories into broader, more general units via explicit supervision. However, this explicit supervision need not be provided for every example in every cluster. Instead, if the clusters are sufficiently pure, we can simply request a label for a single, randomly-selected cluster constituent and propagate that label to the cluster cohabitants. This strategy defines an active learning procedure that requires no pre-existing classifier.

There is natural trade-off between cluster purity and semantic fragmentation in the discovery of categorical structure in a representational space. On one extreme, each data point can be assigned its own category, achieving perfect purity, but with maximal fragmentation. On the other extreme, where all points are placed into one bin, all examples for each class are collocated, but there is no semantic discrimination whatsoever. In the context of a cluster-based active learning procedure, the concepts of purity and fragmentation translate into resulting label noise (precision) and label quantity (recall) for each given cluster labeling budget, a trade-off we explore. Note we found that alternative schemes of labeling more than one example per cluster (and thus, fewer clusters) were not as effective as simply labeling more clusters with the same budget.

Once we have performed this labeling procedure, we will have a collection of labeled examples, which we split into batches of the form  $Z = \{(x_i, y_i)\}_{i=1}^B$ , where each  $x_i \in \mathbb{R}^{F \times T}$  and  $y_i \in \{0, 1\}^C$  for a  $C$ -way classification task (see the yellow path in Figure 1). We can then define our training objective as

$$\mathcal{L}_{\text{class}}(Z) = \frac{1}{B} \sum_{i=1}^B H[y_i, p_{\text{class}}(f(x_i))], \quad (3)$$

where  $p_{\text{class}}: \mathbb{R}^d \rightarrow [0, 1]^C$  is the  $C$ -way output distribution of a classification network operating on the learned audio embeddings and  $H[\cdot, \cdot]$  denotes the cross entropy between labels and predictions.

Finally, it is worth noting that most unsupervised representation learning studies evaluate the utility of the learned embeddings in a lightly supervised classification evaluation, which assumes a small sample of labeled examples with relatively uniform class representation. However, these studies never account for where that small labeled dataset came from. If provided an unbiased sample for annotation, natural class skew will mean oversampling of common classes and the potential to miss some classes entirely. The cluster-based active learning procedure described above is a natural solution to this problem as well.

### 3.4. Learning Curriculum

Jointly optimizing the four objectives listed above, each of which involves specialized auxiliary networks, proves challenging with stochastic gradient descent optimization. Therefore, we devised a

staged learning curriculum that applies the objectives in sequence, first with unsupervised losses in descending order of learning signal, followed by the supervised loss to produce a classifier after labeling. Specifically, we begin by minimizing  $\mathcal{L}_{AV}$  of Equation 2 until convergence. Next, we continue by minimizing the joint AV and AA coincidence loss

$$\mathcal{L}_{\text{coin}} = (1 - \alpha)\mathcal{L}_{AV} + \alpha\mathcal{L}_{AA},$$

where  $\alpha \in [0, 1]$  is an interpolation constant hyperparameters and  $\mathcal{L}_{AA}$  is given by Equation 1. We then introduce the clustering objective and minimize the joint unsupervised loss

$$\mathcal{L}_{\text{joint}} = (1 - \beta)\mathcal{L}_{\text{coin}} + \beta\mathcal{L}_{\text{clust}},$$

where  $\beta \in [0, 1]$  is another interpolation hyperparameter. Finally, after cluster-based labeling, we fine-tune the embedding model,  $f$ , using only the classifier objective,  $\mathcal{L}_{\text{class}}$  of Equation 3.

## 4. EXPERIMENTS

We evaluate our proposed learning framework using the AudioSet dataset [35], consisting of over 2 million video clips, each approximately 10 seconds in duration and labeled using an ontology of 527 audio classes. In contrast to most past studies that use the dataset, we use both the audio and video, sampling at 1 Hz both the image frames (scaled to  $W = H = 128$  pixels and color depth  $D = 3$ ) and log mel spectrogram (25 ms Hanning window, 10 ms step) context windows represented as  $F = 64$  mel bins by  $T = 96$  STFT frames (for a duration of 0.96 s). Due to its proven success in past audio modeling research [36, 11], we use the ResNet-50 architecture for the audio embedding networks ( $f$ ), with the final average pool followed by a  $d = 128$ -dimensional embedding layer. For simplicity we use the identical architecture for the image network ( $g$ ), changing only the input size to match the image dimensions.

Both coincidence prediction networks,  $p_{AA}$  and  $p_{AV}$ , are defined by a single 512-unit fully connected ReLU layer followed by a binary classification output layer (i.e., logistic regression). Each cluster network ( $p_{\text{clust}}$ ) is a single fully connected layer with  $K$  outputs, followed by a softmax nonlinearity to produce probabilities. To improve compatibility with our learned embeddings, which are amenable to cosine distance, we follow [32] by length normalizing both input embeddings and layer weights for each output logit and introduce a fixed logit scaling factor of 60 before applying the softmax. We use diversity hyperparameter  $\gamma = 1.1$  for all clustering models and learning curriculum hyperparameters  $\alpha = \beta = 0.1$  for all experiments so that stronger self-supervised learning criteria dominate. (Note that downstream evaluation performance is not highly sensitive to these settings within reasonable ranges). We evaluate our proposed learning framework on both unsupervised audio representation learning and lightly-supervised classification tasks, described in turn below.

### 4.1. Unsupervised Audio Representation Learning

To measure the utility of our unsupervised representations, we reuse the query-by-example (QbE) and shallow classifier evaluation methodology of [11]. This involves training all unsupervised models on the entirety of the AudioSet training set, while ignoring the labels. Performance is characterized relative to the raw spectrogram features (baseline) and the fully-supervised triplet embedding (topline) from [11], reporting each unsupervised method’s recovery of that range.

The first evaluation is a QbE semantic retrieval task, which directly measures the utility of the distance implied by the learned embedding space. For each class, we compute pairwise cosine distances between a set of positive and negative clips for each class and sort them by ascending distance. We then characterize retrieval performance with the average precision for ranking within-class pairs higher. The second evaluation is classification with a simple architecture, where the entire labeled AudioSet is used to train a 527-way classifier with one 512-unit hidden layer taking the fixed embedding as input. While this simple classifier is fully supervised, it benchmarks the utility of each embedding model as a fixed representation for downstream supervised semantic classification tasks.

Table 1 shows the performance for the (a-b) baseline and topline; (c) the temporal proximity-based unsupervised triplet embedding from [11], which is a state-of-the-art audio-only unsupervised embedding technique; (d) our implementation of the AV correspondence audio embedding [12], where we follow the original recipe that uses VGG architecture, random negative sampling, and  $\Delta T = 1$  s; (e-f) the AA and AV coincidence embeddings that use objectives  $\mathcal{L}_{AA}$  and  $\mathcal{L}_{AV}$  separately, along with ResNet-50 and  $\Delta T = 10$ s; (g-i) AV coincidence ablation experiments to characterize our changes to the original AV correspondence recipe; and (j-k) the joint AV+AA coincidence loss, both with ( $\mathcal{L}_{\text{joint}}$ ) and without ( $\mathcal{L}_{\text{coin}}$ ) the cluster loss (in this case using  $K=1$  million output clusters).

AA coincidence matches the earlier temporal proximity triplet approach for QbE, though there is a moderate loss for shallow model training. The AV correspondence recipe from [12] gives large improvements over all audio-only models (absolute 20% and 9% recovery for QbE and classification, respectively), confirming the power of cross-modal self-supervision demonstrated in that previous work. However, our generalization to AV coincidence provides substantial improvements over the AV correspondence recipe (12% and 9% absolute recovery gain), with both the ResNet-50 upgrade and all-pairs batch construction providing lift in one or both tasks. The increase of coincidence time scale to  $\Delta T = 10$  s performs equivalently to using overlapping AV frames. This indicates the constraint of direct correspondence proposed in [12] is unnecessary for semantic cross-modal AV learning, allowing us to unify the time scale with AA coincidence, which requires longer time scales for success. We find that joint training provides additional gains: the coincidence and clustering objective combination more than doubles the audio-only model recovery for QbE while nearly matching the fully supervised triplet model as a representation for downstream supervised classification tasks.

### 4.2. Sound Classification with Active Learning

Next we evaluate the cluster-based active learning procedure introduced in Section 3.3. We simulate both random labeling baselines and active learning procedures using the AudioSet labels. To adequately simulate the proposed cluster labeling procedure, we must reduce to a 115-class, mutually exclusive subset of AudioSet ontology for the remaining experiments, which guarantees all examples are fully annotated. However, since the labels apply at the clip-level, restricting to this class subset will still bring along a substantial amount of out-of-set audio, making our simulation a worst-case approximation to the real problem.

We first measure intrinsic performance of the clustering method presented in Section 3.2. Table 2 shows the context-window clustering performance in terms of V-Measure (VM) [37], a standard clustering metric, along with the corresponding label precision and recall resulting from the cluster-based labeling procedure. Since the

**Table 1.** Performance of segment retrieval and shallow model classification with fixed representations. All embedding models use ResNet-50 with  $d = 128$ ,  $\Delta T=10$  s, and all-pairs batches (unless noted).

Representation	QbE Retrieval		Classification	
	mAP	recovery	mAP	recovery
a. Explicit Label Triplet (topline)	0.784	100%	0.288	100%
b. Log Mel Spectrogram (baseline)	0.421	0%	0.065	0%
c. Temporal Proximity Triplet [11]	0.549	35%	0.226	72%
d. AV Correspondence (VGG) [12]	0.625	56%	0.249	83%
e. AA Coincidence ( $\mathcal{L}_{AA}$ )	0.552	36%	0.206	63%
f. AV Coincidence ( $\mathcal{L}_{AV}$ )	0.669	68%	0.269	92%
· g. ResNet $\rightarrow$ VGG	0.629	57%	0.265	90%
· h. All-pairs $\rightarrow$ random negatives	0.641	61%	0.253	84%
· i. $\Delta T=10$ s $\rightarrow$ 1 s	0.659	66%	0.270	92%
j. AA+AV Coincidence ( $\mathcal{L}_{coin}$ )	0.677	71%	0.282	97%
k. AA+AV Coincidence + Cluster: $K=1M$ ( $\mathcal{L}_{joint}$ )	0.705	78%	0.285	99%

**Table 2.** Clustering performance and corresponding cluster-based label quality.

$K$	# Active	VM	# Labeled	Recall	Precision
1K	968	0.553	370	0.269	0.097
10K	7,575	0.639	3,700	0.417	0.118
100K	35,830	0.668	35,830	0.560	0.109
1M	77,614	0.674	37,000	0.549	0.117

**Table 3.** Classifier performance for random and cluster labeling.

Label Strategy	Label Budget	Examples w/ Labels	mAP	$d'$
Complete (topline)	3.7M	3.7M	0.566	2.58
Random	370M	370K	0.421	2.28
	185M	185K	0.350	1.96
	74K	74K	0.246	1.71
	37K	37K	0.211	1.56
	3.7K	3.7K	0.083	1.00
	370	370	0.028	0.44
Cluster: $K=1M$	37K	3.3M	0.335	2.15
Cluster: $K=10K$	3.7K	3.0M	0.267	1.80
Cluster: $K=1K$	370	2.7M	0.150	1.10

clustering model is trained on the entirety of AudioSet but evaluated on the mutually exclusive 115-class subset that excludes the high-prior speech and music classes, growth in active clusters is sub-linear in  $K$ . We also see that VM plateaus, indicating the additional finer grained partitioning is not focused on the 115 target classes but instead the background sounds in the evaluation segments. As we increase  $K$  and correspondingly increase the number of clusters labeled, we observe marked improvements to the label recall for a roughly fixed precision (which is limited by the clip-level nature of AudioSet labels). By labeling 37K examples, each representing a distinct cluster, we are able to recover on average half of the positive example labels for the 115-class set with an amount of label noise that is roughly in line with the weakness of the clip-level labels we are using (i.e., for many classes, the sound event only occupies a portion of the AudioSet clip, which means the example-level ground truth labels we score against are inherently noisy).

Next, we use these cluster-based labels to train classifiers. Table 3 shows the 115-way classifier performance for random example sampling baselines (trained from scratch) and the proposed cluster-

based labeling procedure (trained using the curriculum defined in Section 3.4). Here, we vary annotation budget and measure the resulting clip-level classifier performance (we average 0.96 second frame-level scores for each class across the clip to arrive at the clip-level score, as done in [35]) in terms of mean average precision (mAP) and mean  $d'$  (see [35] for details on this useful, but non-standard, evaluation metric). With a small budget and skewed class prior distributions, random sampling tends to overspend on a common classes, yielding little supervision for rare classes.<sup>1</sup> Guiding the annotator effort via the discovered categorical structure, we can turn as little as 370 annotations into cluster-based labels for well over half the examples in the dataset with improved class coverage. Despite the label noise from cluster label propagation, the improvements over random sampling are dramatic; for fixed annotation budget, mean average precision increases by up to a factor of 5.3x, while  $d'$  increases by up to 0.8 absolute. If targeting a specific classifier performance, our cluster-based labeling procedure reduces the required label budget by approximately 2-20x over the range we evaluated.

## 5. CONCLUSIONS

We have presented and evaluated a novel learning framework for building sound representation and recognition models with only a small number of labeled examples. We demonstrated that, by unifying past self-supervised learning successes into a generalized notion of coincidence prediction, we can learn powerful semantic audio representations that enable a highly efficient use of a given annotation budget. By introducing a neural clustering objective, we can simultaneously partition the space for cluster-based active learning while also improving the semantic structure of the embedding space itself, leading to a new high water mark for unsupervised audio representation learning. Moreover, the cluster-based annotations amplify the impact of each solicited label, producing dramatic classification performance gains over random sampling.

## 6. ACKNOWLEDGMENTS

The authors thank Elad Eban, Malcolm Slaney, and Matt Harvey of Google Research for helpful discussions and feedback.

<sup>1</sup>Note that while we train with very few labeled examples for some random sampling baselines, the ResNet-50 architecture still outperforms smaller architectures, a finding consistent with [11].

## 7. REFERENCES

- [1] J. Law, M. Lee, M. Hülse, and A. Tomassetti, “The infant development timeline and its application to robot shaping,” *Adaptive Behavior*, vol. 19, no. 5, pp. 335–358, 2011.
- [2] Yoichi S., “Experience in early infancy is indispensable for color perception,” *Current Biology*, vol. 14, no. 14, pp. 1267–1271, 2004.
- [3] O. J. Braddick and J. Atkinson, “Infants sensitivity to motion and temporal change,” *Optometry and Vision Science*, vol. 86, no. 6, pp. 577–582, 2009.
- [4] D. R. Mandel, P. W. Juszyk, and D. B. Pisoni, “Infants’ recognition of the sound patterns of their own names,” *Psychological Science*, vol. 6, no. 5, pp. 314–317, 1995.
- [5] E. Dupoux, “Cognitive science in the era of artificial intelligence: A roadmap for reverse-engineering the infant language-learner,” *Cognition*, vol. 173, pp. 43–59, 2018.
- [6] A. Cummings, A. P. Saygin, E. Bates, and F. Dick, “Infants’ recognition of meaningful verbal and nonverbal sounds,” *Language Learning and Development*, vol. 5, no. 3, pp. 172–190, 2009.
- [7] L. Goupil, M. Romand-Monnier, and S. Kouider, “Infants ask for help when they know they don’t know,” *PNAS*, vol. 113, no. 13, pp. 3492–3496, 2016.
- [8] E. V. Clark, *First Language Acquisition*, Cambridge University Press, 2009.
- [9] J. Ganger and M. R. Brent, “Reexamining the vocabulary spurt,” *Developmental Psychology*, vol. 40, no. 4, pp. 621, 2004.
- [10] K. Begus and V. Southgate, “Infant pointing serves an interrogative function,” *Developmental Science*, vol. 15, no. 5, pp. 611–617, 2012.
- [11] A. Jansen, M. Plakal, R. Pandya, D. P. W. Ellis, S. Hershey, J. Liu, R. C. Moore, and R. A. Saurous, “Unsupervised learning of semantic audio representations,” in *Proc. of ICASSP*, 2018.
- [12] R. Arandjelovic and A. Zisserman, “Look, listen and learn,” in *Proc. of ICCV*, 2017.
- [13] J. Cramer, H.-H. Wu, J. Salamon, and J. P. Bello, “Look, listen, and learn more: Design choices for deep audio embeddings,” in *Proc. of ICASSP*, 2019.
- [14] R. Urner, S. Wulff, and S. Ben-David, “PLAL: Cluster-based active learning,” in *Proc. of COLT*, 2013.
- [15] A. Jansen, J. F. Gemmeke, D. P. W. Ellis, X. Liu, W. Lawrence, and D. Freedman, “Large-scale audio event discovery in one million youtube videos,” in *Proc. of ICASSP*, 2017.
- [16] M. Tagliasacchi, B. Gfeller, F. de Chaumont Quitry, and D. Roblek, “Self-supervised audio representation learning for mobile devices,” *arXiv preprint arXiv:1905.11796*, 2019.
- [17] P. Agrawal, J. Carreira, and J. Malik, “Learning to see by moving,” in *Proc. of ICCV*, 2015.
- [18] C. Doersch, A. Gupta, and A. A. Efros, “Unsupervised visual representation learning by context prediction,” in *Proc. of ICCV*, 2015.
- [19] D. Pathak, P. Krahenbuhl, J. Donahue, T. Darrell, and A. A. Efros, “Context encoders: Feature learning by inpainting,” in *Proc. of CVPR*, 2016.
- [20] A. van den Oord, Y. Li, and O. Vinyals, “Representation learning with contrastive predictive coding,” *arXiv preprint arXiv:1807.03748*, 2018.
- [21] H. Mobahi, R. Collobert, and J. Weston, “Deep learning from temporal coherence in video,” in *Proc. of ICML*, 2009.
- [22] C. Redondo-Cabrera and R. Lopez-Sastre, “Unsupervised learning from videos using temporal coherency deep networks,” *Computer Vision and Image Understanding*, vol. 179, pp. 79–89, 2019.
- [23] X. Wang and A. Gupta, “Unsupervised learning of visual representations using videos,” in *Proc. of ICCV*, 2015.
- [24] R. Zhang, P. Isola, and A. A. Efros, “Colorful image colorization,” in *Proc. of ECCV*, 2016.
- [25] S. Gidaris, P. Singh, and N. Komodakis, “Unsupervised representation learning by predicting image rotations,” *arXiv preprint arXiv:1803.07728*, 2018.
- [26] G. Andrew, R. Arora, J. Bilmes, and K. Livescu, “Deep canonical correlation analysis,” in *Proc. of ICML*, 2013.
- [27] D. Harwath, A. Recasens, D. Surís, G. Chuang, A. Torralba, and J. Glass, “Jointly discovering visual objects and spoken words from raw sensory input,” in *Proc. of ECCV*, 2018.
- [28] H. Zhao, C. Gan, A. Rouditchenko, C. Vondrick, J. McDermott, and A. Torralba, “The sound of pixels,” in *Proc. of ECCV*, 2018.
- [29] A. Senocak, T.-H. Oh, J. Kim, M.-H. Yang, and I. S. Kweon, “Learning to localize sound source in visual scenes,” in *Proc. of CVPR*, 2018.
- [30] J. S. Chung and A. Zisserman, “Out of time: Automated lip sync in the wild,” in *Proc. of ACCV*, 2016.
- [31] M. Caron, P. Bojanowski, A. Joulin, and M. Douze, “Deep clustering for unsupervised learning of visual features,” in *Proc. of the ECCV*, 2018.
- [32] V. Arora, M. Sun, and C. Wang, “Deep embeddings for rare audio event detection with imbalanced data,” in *Proc. of ICASSP*, 2019.
- [33] J. Xie, R. Girshick, and A. Farhadi, “Unsupervised deep embedding for clustering analysis,” in *Proc. of ICML*, 2016.
- [34] A. Krause, P. Perona, and R. G. Gomes, “Discriminative clustering by regularized information maximization,” in *Advances in Neural Information Processing Systems*, 2010.
- [35] J. F. Gemmeke, D. P. W. Ellis, D. Freedman, A. Jansen, W. Lawrence, R. C. Moore, M. Plakal, and M. Ritter, “Audio Set: An ontology and human-labeled dataset for audio events,” in *Proc. of ICASSP*, 2017.
- [36] S. Hershey, S. Chaudhuri, D. P. W. Ellis, J. F. Gemmeke, A. Jansen, R. C. Moore, M. Plakal, D. Platt, R. A. Saurous, B. Seybold, M. Slaney, R. J. Weiss, and K. Wilson, “CNN architectures for large-scale audio classification,” in *Proc. of ICASSP*, 2017.
- [37] A. Rosenberg and J. Hirschberg, “V-Measure: A conditional entropy-based external cluster evaluation measure,” in *Proc. of EMNLP-CoNLL*, 2007.